

## Interpreting the nonlinear dielectric response of glass-formers in terms of the coupling model

K. L. Ngai

Citation: *The Journal of Chemical Physics* **142**, 114502 (2015); doi: 10.1063/1.4913980

View online: <http://dx.doi.org/10.1063/1.4913980>

View Table of Contents: <http://scitation.aip.org/content/aip/journal/jcp/142/11?ver=pdfcov>

Published by the [AIP Publishing](#)

---

### Articles you may be interested in

[Dynamics of glass-forming liquids. XIX. Rise and decay of field induced anisotropy in the non-linear regime](#)  
*J. Chem. Phys.* **143**, 104504 (2015); 10.1063/1.4929988

[The influence of the secondary relaxation processes on the structural relaxation in glass-forming materials](#)  
*J. Chem. Phys.* **138**, 244502 (2013); 10.1063/1.4811663

[Secondary relaxation processes in binary glass formers: Emergence of “islands of rigidity”](#)  
*J. Chem. Phys.* **138**, 154501 (2013); 10.1063/1.4798655

[Study of the heating effect contribution to the nonlinear dielectric response of a supercooled liquid](#)  
*J. Chem. Phys.* **133**, 234901 (2010); 10.1063/1.3507252

[Dielectric and shear mechanical relaxations in glass-forming liquids: A test of the Gemant-DiMarzio-Bishop model](#)  
*J. Chem. Phys.* **123**, 234510 (2005); 10.1063/1.2136886

---

A promotional banner for AIP Applied Physics Reviews. On the left is a small image of the journal cover, which features a 3D molecular model and the title 'AIP Applied Physics Reviews'. The main part of the banner has a blue background with a bright light source on the right. The text 'NEW Special Topic Sections' is prominently displayed in white. Below this, in an orange section, it says 'NOW ONLINE' in yellow, followed by 'Lithium Niobate Properties and Applications: Reviews of Emerging Trends' in white. The AIP Applied Physics Reviews logo is in the bottom right corner.

**NEW Special Topic Sections**

**NOW ONLINE**  
Lithium Niobate Properties and Applications:  
Reviews of Emerging Trends

**AIP** Applied Physics Reviews

# Interpreting the nonlinear dielectric response of glass-formers in terms of the coupling model

K. L. Ngai

CNR-IPCF, Largo Bruno Pontecorvo 3, I-56127 Pisa, Italy and Dipartimento di Fisica, Università di Pisa, Largo B. Pontecorvo 3, I-56127 Pisa, Italy

(Received 14 November 2014; accepted 20 February 2015; published online 18 March 2015)

Nonlinear dielectric measurements at high electric fields of glass-forming glycerol and propylene carbonate initially were carried out to elucidate the dynamic heterogeneous nature of the structural  $\alpha$ -relaxation. Recently, the measurements were extended to sufficiently high frequencies to investigate the nonlinear dielectric response of faster processes including the so-called excess wing (EW), appearing as a second power law at high frequencies in the loss spectra of many glass formers without a resolved secondary relaxation. While a strong increase of dielectric constant and loss is found in the nonlinear dielectric response of the  $\alpha$ -relaxation, there is a lack of significant change in the EW. A surprise to the experimentalists finding it, this difference in the nonlinear dielectric properties between the EW and the  $\alpha$ -relaxation is explained in the framework of the coupling model by identifying the EW investigated with the nearly constant loss (NCL) of caged molecules, originating from the anharmonicity of the intermolecular potential. The NCL is terminated at longer times (lower frequencies) by the onset of the primitive relaxation, which is followed sequentially by relaxation processes involving increasing number of molecules until the terminal Kohlrausch  $\alpha$ -relaxation is reached. These intermediate faster relaxations, combined to form the so-called Johari-Goldstein (JG)  $\beta$ -relaxation, are spatially and dynamically heterogeneous, and hence exhibit nonlinear dielectric effects, as found in glycerol and propylene carbonate, where the JG  $\beta$ -relaxation is not resolved and in D-sorbitol where it is resolved. Like the linear susceptibility,  $\chi_1(f)$ , the frequency dispersion of the third-order dielectric susceptibility,  $\chi_3(f)$ , was found to depend primarily on the  $\alpha$ -relaxation time, and independent of temperature  $T$  and pressure  $P$ . I show this property of the frequency dispersions of  $\chi_1(f)$  and  $\chi_3(f)$  is the characteristic of the many-body relaxation dynamics of interacting systems which are governed solely by the intermolecular potential, and thermodynamic condition plays no role in this respect. Although linked to  $\chi_3(f)$ , dynamic heterogeneity is one of the parallel consequences of the many-body dynamics, and it should not be considered as the principal control parameter for the other dynamic properties of glassforming systems. Results same as  $\chi_3(f)$  at elevated pressures had been obtained before by molecular dynamics simulations from the four-points correlation function and the intermediate scattering function. Naturally all properties obtained from the computer experiment, including dynamics heterogeneity, frequency dispersion, the relation between the  $\alpha$ - and JG  $\beta$ -relaxation, and the breakdown of the Stokes-Einstein relation, are parallel consequences of the many-body relaxation dynamics governed by the intermolecular potential. © 2015 AIP Publishing LLC. [<http://dx.doi.org/10.1063/1.4913980>]

## I. INTRODUCTION

Recently, nonlinear dielectric response of glassforming matter has become an active research area involving a variety of experimental methods<sup>1–11</sup> and theoretical considerations.<sup>12–14</sup> There are several developments of interest to the present paper. One is the cooperative or correlation length of the structural  $\alpha$ -relaxation, which can be obtained by measurements of the third order dielectric susceptibility  $\chi_3(f)$ .<sup>2–4</sup> Another is the nonlinear contributions to the dielectric permittivity found to be directly related to the heterogeneous dynamics of the structural  $\alpha$ -relaxation.<sup>1,15</sup> These studies were focused on the structural  $\alpha$ -relaxation, which give rise to viscous flow, if the glassformer is not polymeric. There was no experimental study on the nonlinear response of processes

much faster than the  $\alpha$ -relaxation until very recently.<sup>6–10</sup> These experimental investigations might be motivated by the cumulated findings of the relevance of the faster processes to a fundamental solution of the glass transition problem.<sup>16–27</sup> For glass-formers without a resolved secondary relaxation such as glycerol and propylene carbonate, the immediate faster process is the excess wing (EW),<sup>18–21,28–32</sup> which shows up in the dielectric loss,  $\varepsilon''(f)$ , as a second power law of frequency  $f$  at the high frequency flank of the  $\alpha$ -loss peak, i.e.,  $\varepsilon''(f) = A(T)f^{-c}$  with  $c$  approximately about 0.5. By lowering temperature  $T$  to approach or to fall below the glass transition temperature  $T_g$ , another power law with small value of the exponent  $c$  appears at even higher frequencies and is appropriately referred to as the nearly constant loss (NCL). The NCL also can be seen at high frequencies and

temperatures significantly above  $T_g$ .<sup>33–38</sup> References 33, 35, and 37 are optical heterodyne detected optical Kerr effect (OHD-OKE) experiments. The measured quantity is the time derivative of the polarizability–polarizability correlation function, which is equivalent to the time derivative of the orientational correlation function. The OHD-OKE signal  $S(t)$  is related to the susceptibility spectrum by a Fourier transform.<sup>37</sup> Therefore, the observed time dependence of  $S(t) \propto t^{-1+c}$  with  $c \ll 1$  at short times<sup>33,35,37</sup> corresponds exactly to the NCL spectrum in the susceptibility. References 34 and 36 are susceptibility data of amorphous polymers showing directly the NCL in the frequency domain. There is no difference in physics between non-polymeric and polymeric glassformers when confined to the discussion of the structural  $\alpha$ -relaxation, the JG  $\beta$ -relaxation, and the NCL.<sup>23,30</sup>

In another class of glassformers, the relevant faster process is a resolved secondary relaxation with properties showing strong connection to the  $\alpha$ -relaxation,<sup>16,19,22–30</sup> and even faster is the NCL at higher frequencies.<sup>30</sup> Obviously, these properties imply fundamental importance of the secondary relaxations, and they are called<sup>16,22</sup> the Johari-Goldstein (JG)  $\beta$ -relaxation<sup>39</sup> in order to distinguish them from the intramolecular secondary relaxations of no fundamental importance, and at the same time to honor Johari and Goldstein for their important discovery of the existence of a secondary relaxation in a totally rigid molecular glassformer. The coupling model (CM)<sup>16,22–30,40</sup> is the only theoretical framework in the literature that gives a semi-quantitative relations between the NCL of caged dynamics, the JG  $\beta$ -relaxation (more precisely the primitive relaxation in the CM to be defined by Eq. (2) given below), and the  $\alpha$ -relaxation, which are consistent with experiments performed in a variety of glassformers at ambient and elevated pressures. The many-body dynamics in the CM evolve with time. First are the dynamics of caged molecules, manifested as the NCL and caused by the anharmonicity of the intermolecular potential. Second is the primitive relaxation, which terminates the NCL regime.<sup>28–30</sup> The primitive relaxation is followed by the spatially and dynamically heterogeneous relaxation processes (collectively considered as the JG  $\beta$ -relaxation), which involves participations of increasing number of molecules with increase of time. Thus, the JG  $\beta$ -relaxation is spatially and dynamically heterogeneous as well as to some extent cooperative, consistent with results from simulations.<sup>41</sup> Finally comes the terminal  $\alpha$ -relaxation, which has the Kohlrausch time dependence for its correlation function,

$$\phi(t) = \exp[-(t/\tau_\alpha)^{1-n}]. \quad (1)$$

Incidentally, the sequence of processes in the CM given in the above is somewhat similar to the one hinted by the schematic Figure 2 in the review article of Lunkenheimer *et al.*<sup>18</sup> The primitive relaxation time,  $\tau_0$ , can be obtained at temperature  $T$  and pressure  $P$  from  $\tau_\alpha$  and  $(1-n)$  of the Kohlrausch function in Eq. (1) via the time honored coupling model relation,<sup>30,40</sup>

$$\tau_\alpha(T, P) = [t_c^{-n} \tau_0(T, P)]^{1/(1-n)}, \quad (2)$$

where  $t_c = 1\text{--}2$  ps for molecular glassformers. The many-body nature of the  $\alpha$ -relaxation spawns several parallel consequences, not only the Kohlrausch function but also the

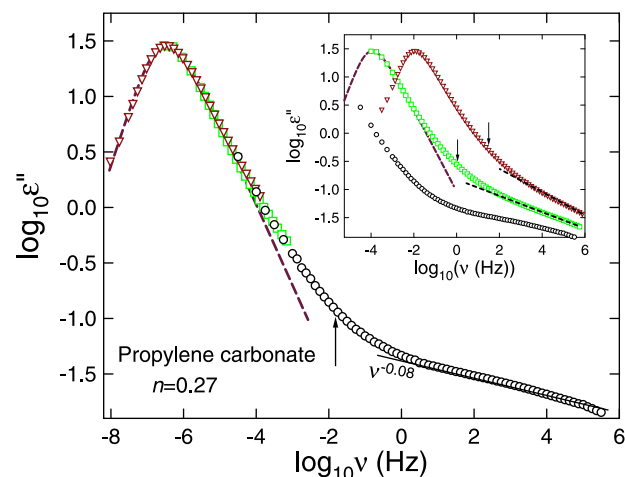


FIG. 1. The inset shows the dielectric loss data of propylene carbonate taken from Schneider *et al.*<sup>20</sup> at three temperatures, 152 K, 155 K, and 158 K and redrawn as a new figure. The data at 152 K were obtained after ageing to achieve thermodynamic equilibrium. The curve is fitted to the  $\alpha$ -relaxation peak by the one-sided Fourier transform of the Kohlrausch function with  $n = 0.27$ . Each vertical arrow pointing towards certain data taken at some temperature indicates the location of the independent relaxation frequency,  $\nu_0$ , calculated for that temperature. The main figure shows the master curve obtained by shifting the data at the two higher temperatures to superpose on the data at the lowest temperature 152 K. The vertical arrow indicates the location of the independent relaxation frequency,  $\nu_0$ , calculated. The dashed line with frequency dependence,  $\nu^{-0.08}$  indicates the slow variation of  $\epsilon''$  at high frequencies or the NCL regime. The labels EW and NCL indicate, respectively, the unresolved JG  $\beta$ -relaxation and the caged molecules dynamics regime.

dynamic heterogeneity, and other properties.<sup>30,42</sup> Also  $\tau_0(T, P)$  is approximately equal to the JG  $\beta$ -relaxation time,  $\tau_{JG}(T, P)$ , i.e.,  $\tau_{JG}(T) \approx \tau_0(T)$ , as found in many glassformers.<sup>16,22–30</sup> The prediction that  $\tau_0(T, P)$  is an upper bound of the NCL time regime has been verified in many molecular glassformers,<sup>28–30</sup> and ionic conductors.<sup>43</sup> For propylene carbonate (PC), this is brought out in Fig. 1 by the dielectric loss spectra, where the vertical arrow indicates the primitive relaxation frequency,  $f_0(T, P) \equiv 1/[2\pi\tau_0(T, P)]$ , and the line is the fit to the Fourier transform of the Kohlrausch function with  $n = 0.27$  (Eq. (1)). Glassformers such as PC and glycerol have no resolved secondary relaxation either in the equilibrium liquid state or in the glassy state because  $f_{JG}(T) \equiv 1/[2\pi\tau_{JG}(T)]$  is located too close to  $f_\alpha(T)$ , as suggested by the location of  $\log f_0(T)$  in Fig. 1 and the approximate relation  $f_0(T) \approx f_{JG}(T)$  in the CM. This approximate relation helps to define  $f_{JG}(T)$  for those glassformers where the JG  $\beta$ -relaxation is not resolved. In the frequency range bounded by  $f_0(T) \approx f_{JG}(T)$  and the frequency at the onset of deviation of the  $\epsilon''(f)$  data from the Kohlrausch fit, the slope,  $d \log \epsilon''(f)/d \log f$  varies within the range from 0.50 to 0.40. This region is designated the EW in the CM. At still higher frequencies is the NCL with the power law dependence,  $\epsilon''(f) = A(T)f^{-c}$ , where  $c$  is a small positive number, decreasing on decreasing temperature as can be seen from the inset of Fig. 1. The  $\epsilon''(f)$  data in this region originate from the motion of molecules that are mutually caged via the intermolecular potential. Unlike true relaxation, the NCL with power law frequency dependence has no characteristic time constant. It persists to lower frequencies until its cutoff frequency  $f_{NCL}(T)$  is reached, beyond which caged dynamics

are terminated by the JG  $\beta$ -relaxation, and the power law dependence of  $\varepsilon''(f)$  no longer holds. The lower bound of the NCL regime,  $f_{\text{NCL}}(T)$ , is higher than  $f_0(T) \approx f_{\text{JG}}(T)$ , and the separation between  $f_0(T) \approx f_{\text{JG}}(T)$  and  $f_{\text{NCL}}(T)$ , increases with decrease of temperature near  $T_g$  as can be seen from the inset of Fig. 1.

It is necessary to make the premise of the CM clear before applying it to nonlinear response. This is because of the marked difference in the interpretation of the caged dynamics between the CM and the idealized Mode Coupling Theory<sup>17</sup> as well as the specific view of other active contributors to the field. For example, the authors of Ref. 32 proposed the succession of processes appearing in the loss spectra of glycerol and PC on increasing frequency are the  $\alpha$ -relaxation, an EW, and the  $\beta$ -relaxation (see, e.g., Fig. 5 in Ref. 32(b)). This view is in stark contrast to the CM, which has the EW representing the unresolved JG  $\beta$ -relaxation to be followed by the NCL at higher frequencies. The view of the EW by Bauer *et al.*<sup>7</sup> as due to a secondary relaxation is the same as the CM, but they made no clear distinction of it from the NCL at higher frequencies. The Appendix gives more details of the CM and justification of its interpretation of the EW, the JG  $\beta$ -relaxation and the NCL, and the multiple connections between the JG  $\beta$ -relaxation and the  $\alpha$ -relaxation,<sup>16,19,22–30,44–48</sup> all of which are relevant for the discussion of the nonlinear dielectric effects<sup>7–10</sup> and the isochronal superposition<sup>11</sup> of the third-order susceptibility  $\chi_3(f)$  independent of pressure and temperature at constant  $\tau_\alpha(T, P)$  in the following sections.

The purpose of the present work is to bring back the recent nonlinear response and nonlinear susceptibility measurements at ambient<sup>7–10</sup> and elevated pressures,<sup>11</sup> and examine consistency of the data with the interpretations of the dynamics from the CM when extended to the nonlinear regime.

## II. NONLINEAR CONTRIBUTIONS TO THE PERMITTIVITY

### A. Glassformers having no resolved secondary relaxation

Starting from the measurements of the nonlinear contributions to the dielectric permittivity of glycerol and propylene glycol by Richert and Weinstein,<sup>1,15</sup> the results were found to be directly related to the heterogeneous dynamics of the  $\alpha$ -relaxation. The findings reinforce the previous evidences of heterogeneous  $\alpha$ -dynamics by multidimensional nuclear magnetic resonance<sup>49</sup> and by dielectric hole burning.<sup>50</sup> The latter technique was applied to glycerol and propylene carbonate by Schiener *et al.*<sup>50</sup> in the viscous regime near  $T_g$ . It was also used to find heterogeneous dynamics of the ion diffusivity in glassy  $2\text{Ca}(\text{NO}_3)_2 \cdot 3\text{KNO}_3$  (CKN),<sup>51</sup> in the JG  $\beta$ -relaxation of glassy D-sorbitol,<sup>52</sup> and in the high frequency flank of supercooled glycerol.<sup>53</sup> According to the CM, the ion conductivity of ionic conductors containing high density of ions such as in CKN is also non-exponential, cooperative, and dynamically heterogeneous,<sup>54</sup> and these properties have support from simulations.<sup>55</sup>

An important advance of the nonlinear dielectric measurements of glass-forming glycerol and propylene carbonate was

made by Bauer *et al.*<sup>7</sup> and Samanta and Richert.<sup>9</sup> These authors have extended the measurement at high electric field to sufficiently high frequencies to allow them to investigate the nonlinear behavior of the EW, and the NCL. It is worth mentioning that dielectric hole burning experiments also found different behavior of the persistence time of the burned holes in glycerol for the EW than the  $\alpha$ -relaxation.<sup>53</sup> The novel and more specific finding by Bauer *et al.* in glycerol and PC is a lack of significant nonlinear behavior in the NCL regime, in contrast to the strong increase of dielectric constant  $\varepsilon'$  and loss  $\varepsilon''$  found for unresolved JG  $\beta$ -relaxation and the  $\alpha$ -relaxation which is in agreement with the earlier high electric field studies of Richert and Weinstein.<sup>1,15</sup> Their data of the increase of  $\varepsilon''$  by the application of the high field  $E$ ,  $\Delta \log \varepsilon''(E, f) = \log \varepsilon''(E, f) - \log \varepsilon''(14 \frac{\text{kV}}{\text{cm}}, f)$ , are reproduced in Figs. 2 and 3 for glycerol and PC, respectively, to facilitate further discussion of the data, and interpretation from the CM recapitulated in the Introduction and elaborated in the Appendix. The NCL represents the dielectric loss  $\varepsilon''$  showing up as a second power law  $A(T)f^{-c}$  with small value of  $c$  at frequencies beyond the high-frequency flank of the  $\alpha$ -loss peak, as indicated by the dashed line in Fig. 2 of glycerol for 186 K, and in Fig. 3 of PC at 158 K. The slopes of the dashed lines determine the value of  $c \approx 0.2$ . As discussed in the Introduction, the terminology, EW, in this case should be changed to NCL because of the small value of  $c$ . The origin of EW or NCL was interpreted by some as due to an unresolved secondary relaxation<sup>20,21,56</sup> or specifically an unresolved JG  $\beta$ -relaxation.<sup>57</sup> Another interpretation is that it is a part of the  $\alpha$ -relaxation.<sup>58</sup> It is not clear how these views of the EW can explain its lack of significant increase of  $\Delta \log \varepsilon''(E, f)$ , which is a general property since the same was observed in glycerol and PC. For this reason, Bauer *et al.*<sup>7</sup> declared that this finding is unexpected or surprising, and thus it challenges for an explanation.

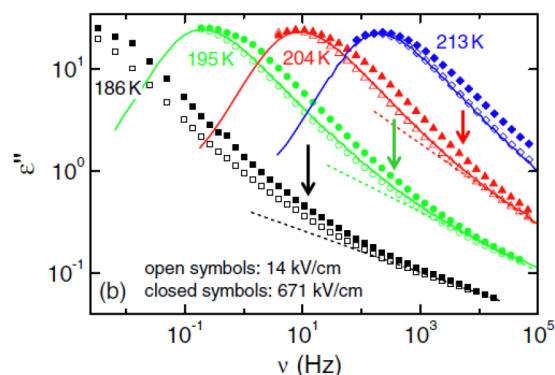


FIG. 2. Data are  $\varepsilon''$  of glycerol reproduced from Th. Bauer, P. Lunkenheimer, S. Kastner, and A. Loidl, Phys. Rev. Lett. **110**, 107603 (2013). Copyright 2013 by American Physical Society. Added are the primitive relaxation frequencies at three temperatures indicated by the arrows. The dashed lines located at the high frequency end of the data have small slope and correspond to the NCL. Open and closed symbols are measured values at fields of 14 kV/cm and 671 kV/cm, respectively. The solid lines correspond to data previously published in Ref. 20, and measured at 0.2 kV/cm. Adapted with permission from Th. Bauer, P. Lunkenheimer, S. Kastner, and A. Loidl, Phys. Rev. Lett. **110**, 107603 (2013). Copyright 2013 by American Physical Society.



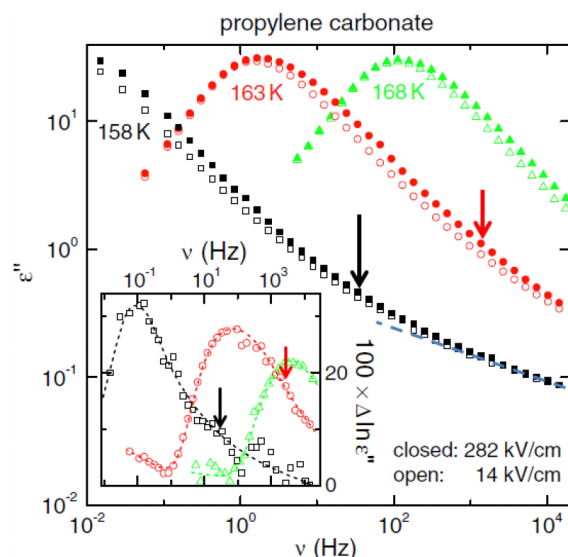


FIG. 3. Data are  $\epsilon''$  of PC reproduced from Th. Bauer, P. Lunkenheimer, S. Kastner, and A. Loidl, Phys. Rev. Lett. **110**, 107603 (2013). Copyright 2013 by American Physical Society. Added are the primitive relaxation frequencies at three temperatures indicated by the arrows. Open and closed symbols are measured values at fields of 14 kV/cm and 282 kV/cm, respectively. The blue dashed line located at the high frequency end of the data at 158 K has small slope and corresponds to the NCL. The inset shows the difference of the logarithm of the loss spectra shown in the main frame. Added are the primitive relaxation frequencies at two temperatures indicated by the arrows. The lines are guides for the eyes. Adapted with permission from Th. Bauer, P. Lunkenheimer, S. Kastner, and A. Loidl, Phys. Rev. Lett. **110**, 107603 (2013). Copyright 2013 by American Physical Society.

In advancing the explanation by the CM based on the evolution of many-body relaxation with time, the primitive relaxation time,  $\tau_0(T)$ , is calculated from Eq. (2) with  $t_c = 2$  ps for glycerol and PC. The values of  $\tau_\alpha(T)$  and the temperature independent value of  $(1 - n)$  at temperatures near  $T_g$  are obtained from the fit of the  $\alpha$ -loss peak by the Fourier transform of the Kohlrausch function in Eq. (1). From the calculated values of  $\tau_0(T)$ , the corresponding primitive frequency,  $f_0(T) \equiv 1/(2\pi\tau_0(T))$ , are indicated by the arrows in Figs. 2 and 3. For glycerol at 186 and 195 K, it can be seen by inspection of Fig. 2 that  $f_0(T)$  is about one decade or so lower than the cutoff frequency  $f_{NCL}$  of the power law  $A(T)f^{-c}$ . The latter is therefore the NCL of caged molecule according to the CM, which is terminated by the onset of the primitive relaxation. As mentioned before in the Introduction, the caged molecules regime is neither a relaxation process nor a distribution of relaxation processes. Instead, the NCL originates from the anharmonicity of the intermolecular potential confining the molecules mutually within cages. As long as the intermolecular potential is not modified by the applied high electric field, there is no change of the NCL from the caged molecules either. Therefore, by correctly identifying the EW as the NCL of caged molecules in the CM, but not as a distribution of relaxations, the lack of significant change of  $\Delta \log \epsilon''(E, f)$  in the NCL regime observed by Bauer *et al.*<sup>7</sup> is explained.

After the NCL regime is terminated by the onset of the primitive relaxation with frequency  $f_0(T)$ , the evolution of many-body relaxation takes over. As discussed in more detail in the Appendix, starting from the primitive relaxation,

the time evolution consists of a sequence of heterogeneous relaxation processes (collectively called the JG  $\beta$ -relaxation whether it is resolved or not) involving more and more molecules, and becoming increasingly more heterogeneous and cooperative, and terminating with the Kohlrausch  $\alpha$ -relaxation. Richert and Weinstein<sup>1,15</sup> found nonlinear contributions to the permittivity to be directly related to the heterogeneous relaxation. Thus, nonlinear dielectric effect in terms of  $\Delta \log \epsilon''(E, f)$  is expected from this sequence of heterogeneous processes at lower frequencies than the primitive relaxation frequency  $f_0(T)$ . At the present time, there is no theory including the CM that can relate the heterogeneity of a process and the number of molecules involved to the  $\Delta \log \epsilon''(E, f)$  measured. Nevertheless, it is reasonable to assume the process that is more heterogeneous and involving more molecules corresponds to larger  $\Delta \log \epsilon''(E, f)$ . If this assumption is valid, then the dynamics envisaged in the CM is fully consistent with the observed monotonic increase of  $\Delta \log \epsilon''(E, f)$  with decreasing frequency starting from the primitive relaxation frequency, as shown in Figs. 2 and 3. Justification of the assumption may be based on the work of Richert and Weinstein.<sup>1</sup> They have already found that the nonlinear contributions to the permittivity are directly related to the heterogeneous distribution of relaxation times.

Nonlinear dielectric effects on various processes, including the caged molecule dynamics, the sequence of heterogeneous processes constituting the JG  $\beta$ -relaxation, and the structural  $\alpha$ -relaxation, are all different. Elucidation of the differences in size of the nonlinear effect of these processes, and the increase of  $\Delta \log \epsilon''(E, f)$  on decreasing frequency past  $f_0$ , is one of the objectives of this paper. Although increasing number of correlated molecules with increasing heterogeneity in the sequence of processes following the primitive relaxation is expected by the CM, it cannot give quantitatively the number from the frequency dependence of  $\Delta \log \epsilon''(E, f)$  over the entire range from NCL to the JG  $\beta$ -relaxation and the  $\alpha$ -relaxation. No other theory in the literature can do this either. This feat, if accomplished, is tantamount to having the glass transition problem almost solved. The theories based on the work of Bouchaud and Biroli<sup>2-4</sup> were specifically constructed to calculate  $N_{\text{corr}}(T)$  of the  $\alpha$ -relaxation from  $\chi_3(f)$  in nonlinear response experiments. The theories<sup>2-4</sup> are certainly important advances, but so far they have not been developed to address either the nonlinear effect on the NCL and the JG  $\beta$ -relaxation, or the multitude of linear dynamic properties<sup>22-30</sup> in glassformers and non-glassformers. In contrast, the CM is designed to address dynamic properties of interacting systems in general, and glass-forming systems are just a special case. The success of the CM in explaining dynamic properties in various complex interacting systems<sup>30</sup> has not been accomplished by another theory. The present paper addresses aspects of the nonlinear effect related to the NCL and the JG  $\beta$ -relaxation not covered by the theories on nonlinear effects,<sup>2-4,15</sup> and therefore it should be considered as a supplement to these theories.

Samanta and Richert (SR)<sup>9</sup> also have made dielectric relaxation measurements on PC, glycerol, and 2-methyltetrahydrofuran at high electric fields to investigate the nonlinear effect on all the processes including the EW. The

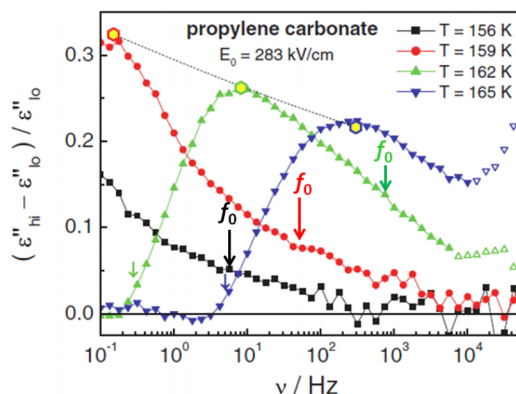


FIG. 4. Data of field induced relative change of the dielectric loss of propylene carbonate plotted against frequency at the temperatures indicated are reproduced from J. Chem. Phys. **140**, 054503 (2014). Copyright 2014 by American Institute of Physics. The subscripts “hi” and “lo” in the label of the ordinate refer to electric fields of  $E = 283$  kV/cm and 14 kV/cm, respectively. Added are the primitive relaxation frequencies  $f_0$  at three temperatures indicated by the longer and thicker arrows. The NCL starting at frequencies higher than  $f_0$  by one decade or more has nearly vanishing nonlinear dielectric effect within experimental uncertainties. For the temperatures of 162 and 165 K, the loss peak frequencies are indicated by shorter and thinner arrows at  $\nu_{\max} = 0.28$  and 5.0 Hz, respectively. Adapted with permission from J. Chem. Phys. **140**, 054503 (2014). Copyright 2014 by American Institute of Physics.

nonlinear dielectric effects given by  $(\varepsilon''_{hi} - \varepsilon''_{lo})/\varepsilon''_{lo}$ , where  $\varepsilon''_{hi}$  and  $\varepsilon''_{lo}$  are the loss measured at high and low fields, respectively, are reproduced in Fig. 4. By the way,  $\Delta \ln \varepsilon''(E, f) = \ln(\varepsilon''_{hi}/\varepsilon''_{lo})$  of Bauer *et al.* is practically the same as  $(\varepsilon''_{hi} - \varepsilon''_{lo})/\varepsilon''_{lo}$  of SR because  $\varepsilon''_{hi}/\varepsilon''_{lo}$  is close to one. Consistent with similar experiments reported by Bauer *et al.*, the values of  $\Delta \log \varepsilon''(E, f)$  approach zero at frequencies exceeding about  $10^5 \omega_{\max}$ . Added in the figure are the calculated  $\log f_0(T)$  at three temperatures, the locations of which are indicated by the arrows. For  $T = 156$  and 159 K, the nonlinear effect becomes small at frequencies starting at about a decade higher than  $\log f_0(T)$ . According to the CM interpretation briefly discussed in the Introduction, the response in this higher frequency region is contributed by the NCL of caged molecules. Thus, as stated by SR in Ref. 9, their data of  $(\varepsilon''_{hi} - \varepsilon''_{lo})/\varepsilon''_{lo}$  obtained after applying the high field for a moderate number of cycles are consistent with the lack of significant change of  $(\varepsilon''_{hi} - \varepsilon''_{lo})/\varepsilon''_{lo}$  in the NCL regime found by Bauer *et al.* in Figs. 2 and 3.

Notwithstanding, SR have the concern that the loss values they obtained after applying the high field for a moderate number of cycles may not reflect the steady state situation. This concern had led SR to perform a time resolved high-field dielectric relaxation measurements at frequencies up to  $10^7$  times the peak frequency  $\omega_{\max}$  of the  $\alpha$ -loss at temperatures  $T$  near and below  $T_g$  in glycerol (e.g.,  $T = 186$  K) and PC (e.g.,  $T = 154$ –156 K). They measured the time dependent relative change of the dielectric loss,  $(\varepsilon''_{hi} - \varepsilon''_{lo})/\varepsilon''_{lo}$ , up to a few hundred seconds at various frequencies in propylene carbonate, 2-methyltetrahydrofuran, and glycerol. SR examined the change with time of the “vertical” difference,  $(\varepsilon''_{hi} - \varepsilon''_{lo})/\varepsilon''_{lo}$ , and fit its time dependence by a stretched exponential function. Moreover, they considered the “horizontal” difference between high and low field losses, defined by

$$\ln \tau_{hi} - \ln \tau_{lo} = [(\varepsilon''_{hi} - \varepsilon''_{lo})/\varepsilon''_{lo}] / [d \ln \varepsilon''_{lo} / d \ln \omega]. \quad (3)$$

They found that  $\ln \tau_{hi} - \ln \tau_{lo}$  requires an unexpectedly long time of the order of the structural relaxation time  $\tau_{\alpha}(T)$  to reach the equilibrium value for all processes faster than the  $\alpha$ -relaxation with angular frequency  $\omega_{\max}$ . From the horizontal difference of PC obtained in the frequency range  $10^4 \leq \omega/\omega_{\max} < 10^7$  at 154 K, and  $10^3 \leq \omega/\omega_{\max} < 3 \times 10^6$  at 155 K, SR made the conclusion: “Therefore, even deep within the excess wing regime, the extent of nonlinearity regarding dielectric polarization is practically as pronounced as for frequencies that are much closer to the loss peak.” On the other hand, Bauer *et al.*<sup>7</sup> made clear in their paper and Supplementary Information that  $\Delta \log \varepsilon''(E, f)$  has reached its steady state value at much shorter times. Reported in the Supplementary Information of their paper,<sup>7</sup> they performed two high-field (565 kV/cm) measurements of glycerol at 186 K, one at the fastest mode possible and the other after many field cycles. Typical numbers of cycles were about 10 cycles for  $f < 1$  Hz, 50 cycles for 100 Hz, 2000 cycles for 1 kHz, and  $\geq 2 \times 10^5$  cycles for 100 kHz. By inspection of the data at 186 K in Fig. 2 herein, it is clear that 100 Hz is near the onset of the NCL, and 1 kHz is already inside the NCL regime. In the frequency region from 100 Hz to 100 kHz, Bauer *et al.* found no difference of  $\varepsilon''_{hi}$  measured by the fast mode and after many cycles. From this result, they concluded that the absence of change of  $\varepsilon''$  with high field in the NCL is not due to a non-equilibrium effect.

The time scale for  $\Delta \log \varepsilon''(E, f)$  to reach steady state in the experiment of Bauer *et al.* is very different than that of SR. Based on their time resolved data, SR stressed that  $\Delta \log \varepsilon''(E, f)$  should be deduced from its long time limit of a few hundred seconds. At the time of writing this paper, Bauer *et al.* still maintain<sup>59</sup> that they have reached steady state in their measurement. Thus, this disparity in results from the two groups cannot be resolved by anyone at this time. It was suggested by a reviewer that the physics probed by the two experimental techniques used by Bauer *et al.* and by SR are quite different, and one cannot properly compare their results, even for the same glassformers, and approximately the same frequency range for the probing electric field used in the two studies. Accepting this suggestion, the steady state data of PC from SR are reexamined here (independently of Bauer *et al.*) to understand better the spectral range covered by the measurements. In the horizontal plot of SR, the absolute value of the denominator,  $d \ln \varepsilon''_{lo} / d \ln \omega$ , on the right-hand-side of Eq. (3) is a monotonic decreasing function of frequency, becoming very small in the NCL region where  $\varepsilon''_{lo} = A(T)f^{-c}$  with  $c \ll 1$ . This can be seen by inspection of the inset in Fig. 1 that at 155 K, the value of  $c$  is less than 0.1. The absolute value of denominator,  $d \ln \varepsilon''_{lo} / d \ln \omega$ , is exactly  $c$  in the NCL regime. It's very small value magnifies the horizontal change,  $\ln \tau_{hi} - \ln \tau_{lo}$ , in the NCL regime ( $\omega \geq \omega_{\text{NCL}}$ ) than the relaxation processes at lower frequencies. Therefore, the question remains is how large the nonlinear effect in the NCL regime when examined in terms of  $(\varepsilon''_{hi} - \varepsilon''_{lo})/\varepsilon''_{lo}$ . In Fig. 5, the 155 K experimental data of  $\varepsilon''_{lo}$  of PC obtained at frequencies closely spaced together<sup>18,20</sup> are differentiated, and the values of  $d \ln \varepsilon''_{lo} / d \ln \omega$  are shown as a function of  $\omega/\omega_{\max}$  by the line. Also shown are the Kohlrausch fit of the  $\alpha$ -relaxation, the location of the normalized primitive relaxation frequency,

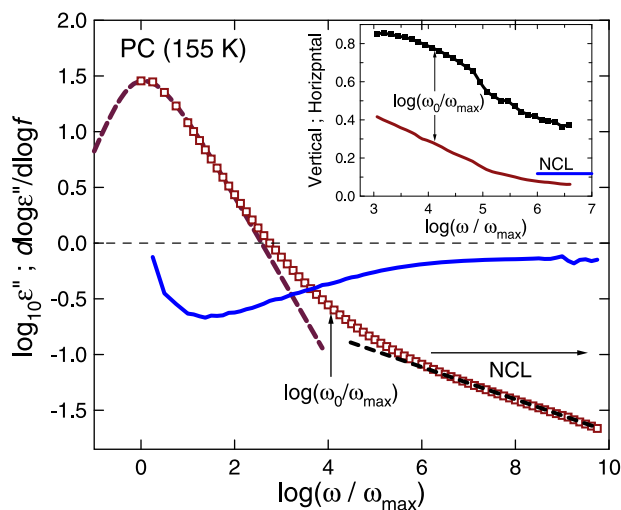


FIG. 5. The blue curve is the derivative,  $d \log \epsilon''_{lo} / d \log(\omega / \omega_{\max})$ , calculated from the low field dielectric loss data (red squares) of PC at 155 K. The power law dependence of NCL is indicated by the back dashed line, and the NCL regime by the horizontal arrow. The location of the normalized primitive frequency,  $\omega_0 / \omega_{\max}$ , is indicated by the vertical arrow. In the inset, the black squares and the red line are, respectively, the horizontal and vertical normalized changes at high field of PC at 155 K. The horizontal data are taken from Ref. 9, and the vertical values are obtained by multiplication with  $d \log \epsilon''_{lo} / d \log(\omega / \omega_{\max})$  in the main figure.

$\omega_0 / \omega_{\max}$ , by the vertical arrow, and the normalized frequency regime of the NCL, identified by the power law dependence of  $A(T)(\omega / \omega_{\max})^{-c}$  and indicated by the horizontal arrow. In the inset, the steady state values of  $\ln \tau_{hi} - \ln \tau_{lo}$  at 155 K and high field of  $E_0 = 283$  kV/cm for PC from SR<sup>9</sup> are shown together with the values of  $(\epsilon''_{hi} - \epsilon''_{lo}) / \epsilon''_{lo}$  calculated from  $\ln \tau_{hi} - \ln \tau_{lo}$  according to Eq. (3). The normalized frequency regime of the NCL is indicated by the blue line drawn starting at the onset normalized frequency,  $\omega_{NCL} / \omega_{\max}$ , exactly the same as in the main part of the figure. It can be seen by inspection of the inset that the steady state data of  $(\epsilon''_{hi} - \epsilon''_{lo}) / \epsilon''_{lo}$  had not been obtained in the NCL regime. Nevertheless, there is a monotonic decrease of  $(\epsilon''_{hi} - \epsilon''_{lo}) / \epsilon''_{lo}$  on increasing  $\omega / \omega_{\max}$  toward  $\omega_{NCL} / \omega_{\max}$ . If this trend continues deeper into the NCL regime, then the small or lack of nonlinear effect of  $(\epsilon''_{hi} - \epsilon''_{lo}) / \epsilon''_{lo}$  of the caged dynamics can be substantiated. Verification or contradiction of this behavior has to wait for measurements of steady state nonlinear effects extended to higher frequencies in the future. High quality experimental data of  $\epsilon''_{lo}$  of glycerol at 186 K are not available from Refs. 18 and 20 to consider the same issue of the steady state nonlinear data of glycerol at 186 K from SR<sup>9</sup> as in the above for PC. However, such data at 185 K are available. The same operation had been performed on the  $\epsilon''_{lo}$  data of glycerol at 185 K as for PC in Fig. 5. The value of  $\log(\omega_{NCL} / \omega_{\max})$  is about 6.5 at 185 K and it is not expected to change much at 186 K, while the steady state horizontal change,  $\ln \tau_{hi} - \ln \tau_{lo}$ , were obtained<sup>9</sup> at 186 K for values of  $\log(\omega / \omega_{\max})$  less than 6. Therefore, higher frequency measurements of the steady state nonlinear effects in glycerol are needed before the behavior of the NCL at high fields can be ascertained.

A comparison of the high-field dielectric relaxation measurements obtained at the quasi-instantaneous condition

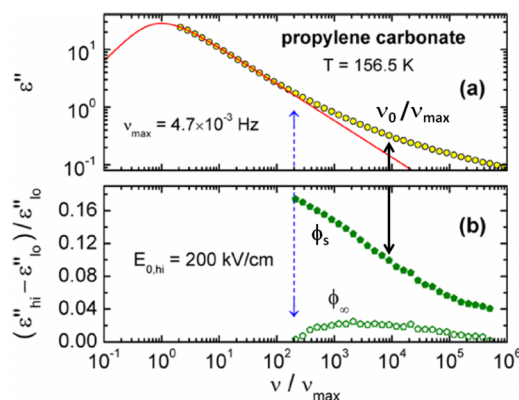


FIG. 6. Dielectric relaxation results for the  $\alpha$ -process of propylene carbonate at a temperature of  $T = 156.5$  K at low and high fields. Reproduced from S. Samanta and R. Richert, J. Phys. Chem. B (to be published). Copyright 2014 by American Chemical Society, and modified to show by the thicker black arrow the location of the calculated value of  $v_0 / v_{\max} \approx 10^4$  in both panels. (a) Experimental data for the low field (linear response) dielectric loss spectrum (symbols), along with an HN fit (line) that is extrapolated to show the loss peak. (b) The “vertical” relative difference,  $(\epsilon''_{hi} - \epsilon''_{lo}) / \epsilon''_{lo}$ , between loss spectra recorded at  $E_{0,hi} = 200$  kV/cm and  $E_{0,lo} = E_{0,hi} / 10$ . Open symbols represent quasi-instantaneous levels,  $\phi_{\infty}$ , while solid symbols are for steady state values,  $\phi_s$ .

and at steady state was presented in a plot of  $(\epsilon''_{hi} - \epsilon''_{lo}) / \epsilon''_{lo}$  versus  $\log(\omega / \omega_{\max})$  by SR<sup>10</sup> for PC at 156.5 K, and reproduced as Fig. 6 herein. The plot shows significant increase in the values of  $(\epsilon''_{hi} - \epsilon''_{lo}) / \epsilon''_{lo}$  in the higher frequencies region measured at steady state than at the quasi-instantaneous condition. The higher frequencies covered extend up to about 5.8 decades higher than the  $\alpha$ -loss peak frequency  $v_{\max}$  at low field and  $T = 156.5$  K, which is estimated to be about  $6.3 \times 10^{-4}$  Hz from the value of  $v_{\max} = 10^{-4}$  Hz at 155 K and the Vogel-Fulcher-Tammann fit in Ref. 20. From this value of  $v_{\max}$ , the primitive frequency  $v_0$  at 156.5 K is calculated and shown by the ratio  $v_0 / v_{\max} \approx 10^4$  in Figs. 6(a) and 6(b). It can be seen from Fig. 6(b) that the data of  $(\epsilon''_{hi} - \epsilon''_{lo}) / \epsilon''_{lo}$  at the high field of 200 kV/cm are available in the scaled frequency range less than 2 decades higher than  $\log(v_0 / v_{\max})$ . Considering the fact that at 155 K, the onset frequency,  $v_{NCL}$ , of the NCL regime is about one and a half decade higher than  $v_0$  as shown in Fig. 4, the paucity of steady state data higher than  $v_{NCL}$  (by only about 0.3 decade) in Fig. 6(b) cannot unequivocally tell the size of the  $(\epsilon''_{hi} - \epsilon''_{lo}) / \epsilon''_{lo}$  at frequencies well inside the NCL regime.

Before closing this subsection, worth mentioning are the NCL and its properties observed by experimental techniques other than dielectric relaxation. These include optical heterodyne-detected optical Kerr effect,<sup>33,35,37</sup> dynamic light scattering,<sup>34,36</sup> quasielastic neutron scattering measurements at times shorter than 1 ns and temperatures below  $T_g$  of glassformers of various kinds,<sup>60–62</sup> and the time resolved mean-square-displacements of colloidal particles by confocal microscopy.<sup>63,64</sup>

## B. Glassformers having a resolved JG $\beta$ -relaxation

Already has been discussed in the Introduction and elaborated in the Appendix, starting from the local primitive



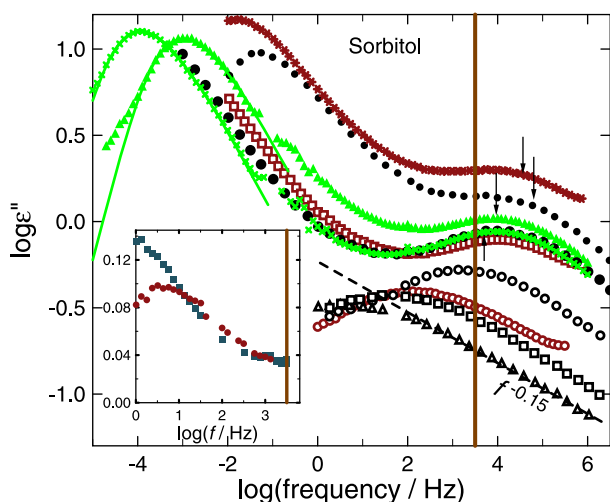


FIG. 7. The inset is a plot of the steady state values  $\phi_s$  vs.  $\log f$  at  $T = 267$  and  $270$  K of D-sorbitol. The results are obtained by digitization of data published in Fig. 3 of Ref. 10. The vertical brown line at  $\log(f/\text{Hz}) = 3.5$  is drawn to indicate no data of  $\phi_s$  were acquired at frequencies higher  $10^{3.5}$  Hz. The same brown line appears in the main figure showing the dielectric loss spectra of D-sorbitol from three different sources. (Black) Kastner *et al.*<sup>31</sup> at temperatures 272, 267, 245, 215, and 200 K (from top to bottom). (Red) Samanta and Richert<sup>10</sup> at 270, 267, and 220 K (from top to bottom) after shifting the data at 270 K vertically upward by 0.30 decade to enhance visibility. (Green) Nozaki *et al.*<sup>66</sup> at 264 and 266 K (from left to right). The fits of the  $\alpha$ -loss peak by the Fourier transform of the Kohlrausch function with  $(1-n) = 0.50$  are shown by the green lines.

relaxation, the so-called JG  $\beta$ -relaxation is actually a collection of relaxation processes, involving increasing number of molecules and degrees of heterogeneity as well as cooperativity with increasing time, occurring before the onset of the terminal Kohlrausch  $\alpha$ -relaxation. From this CM view of the nature of the JG  $\beta$ -relaxation, we can expect significant nonlinear dielectric effects exhibited by the JG  $\beta$ -relaxation in high-field dielectric experiments. The expected nonlinear effects on the resolved JG  $\beta$ -relaxation in high fields were observed in D-sorbitol by SR,<sup>10</sup> and also by Bauer.<sup>65</sup> The steady state values  $\phi_s$  of  $(\epsilon''_{\text{hi}} - \epsilon''_{\text{lo}})/\epsilon''_{\text{lo}}$  at  $T = 267$  and  $270$  K, obtained by SR with  $E_{0,\text{hi}} = 190$  kV/cm and  $E_{0,\text{lo}} = E_{0,\text{hi}}/10$  and shown in their Fig. 3,<sup>10</sup> are reproduced in the inset of Fig. 7 herein. The vertical brown line at  $\log(f/\text{Hz}) = 3.5$  is drawn to indicate no data of  $\phi_s$  were acquired at frequencies higher  $10^{3.5}$  Hz. In the main Fig. 7 are dielectric loss spectra of sorbitol from three groups. The data shown in black at 272, 267, 245, 215, and 200 K (from top to bottom) are taken from the paper by Kastner *et al.*<sup>31</sup> The data in red at 270, 267, and 220 K (from top to bottom) are taken from the paper by SR,<sup>10</sup> with the data at 270 K shifted vertically upward by 0.30 decade to enhance visibility. The data in green at 266 and 264 K are taken from Nozaki *et al.*<sup>66</sup> The fits of the  $\alpha$ -loss peaks by the Fourier transform of the Kohlrausch function in Eq. (1) with  $(1-n) = 0.50$  are shown by the green lines.

All the spectra presented in Fig. 7 show the presence of the JG  $\beta$ -relaxation well resolved and well separated from the  $\alpha$ -relaxation, in contrast to glycerol and PC. From Eq. (2) and the approximate equality,  $\tau_{\text{JG}}(T) \approx \tau_0(T)$ , it follows that  $(\log \tau_\alpha - \log \tau_0)$  and  $(\log \tau_\alpha - \log \tau_{\text{JG}})$  are, respectively, exactly and approximately equal to  $n[\log(\tau_\alpha/t_c)]$ . This expression explains

the larger separation between the  $\alpha$ - and the JG  $\beta$ -relaxation in sorbitol having a larger  $n = 0.50$  than in glycerol and PC with smaller  $n = 0.29$  and  $0.27$ , respectively. Each of the four vertical arrows pointing at a curve is located at  $\log[f_0 = (1/2\pi\tau_0)]$ , where  $\tau_0$  is calculated via Eq. (2) from  $\tau_\alpha$  of that curve, and with  $n = 0.50$  and  $t_c = 2$  ps. Like previously found in many glassformers,<sup>16,22–30,67</sup> the value of  $f_0(T) \equiv 1/(2\pi\tau_0(T))$  for each of the four test cases is near  $f_{\text{JG}}(T)$ , the frequency of the JG  $\beta$ -relaxation loss peak in Fig. 7. The loss data at 245, 220, 215, and 200 K taken in the glassy state show not only the JG  $\beta$ -relaxation but also on its high frequency flank the NCL with the power law dependence,  $\epsilon''(f) = A(T)f^{-c}$  with  $c \ll 1$ . At  $T = 200$  K, the value of  $c$  determined by the slope of the dashed line in Fig. 7 is 0.15. Thus, in sorbitol, the NCL of caged molecule dynamics occurs at higher frequencies (shorter times) than the JG  $\beta$ -relaxation and the primitive relaxation, as expected in general by the CM.

We are now ready to compare the nonlinear dielectric response of sorbitol expected by the CM with the experiments by SR<sup>10</sup> and similar results by Bauer.<sup>65</sup> In the CM, the local primitive relaxation as well as the JG  $\beta$ -relaxation is spatially and dynamically heterogeneous. The latter is a collection of relaxations involving increasing heterogeneity and number of correlated molecules. Hence, starting from the primitive frequency  $f_0(T)$ , the steady state value  $\phi_s$  of  $(\epsilon''_{\text{hi}} - \epsilon''_{\text{lo}})/\epsilon''_{\text{lo}}$  is nonzero and increases monotonically on decreasing frequency. This frequency dependence of  $\phi_s$  from the CM is consistent with the data of SR at 267 and 270 K shown in the inset of Fig. 7. The vertical brown line at  $\log(f/\text{Hz}) = 3.5$  in the inset marks the frequency above which data of  $\phi_s$  have not been acquired by SR. The same brown line in the main part of Fig. 7 indicates that  $\log f_0(T)$  is higher than  $\log(f/\text{Hz}) = 3.5$  at  $T = 267$  and  $270$  K. Therefore, the monotonic increase of  $\phi_s$  with decreasing frequency in the inset is consistent with the CM view of the evolution of dynamics with time. On the other hand, the NCL from caged dynamics is well defined only at significantly higher frequencies than  $f_0(T)$  at  $T = 267$  and  $270$  K. Guided by the brown lines in the inset and the main part of Fig. 7, it is clear that the high field measurements on sorbitol at  $T = 267$  K and temperatures above had not been carried out by SR at frequencies higher than  $f_0(T)$  or  $f_{\text{JG}}(T)$ . Hence, the nonlinear dielectric effects in the NCL regime of sorbitol have not yet been characterized at temperatures near and above  $T_g$ . Until  $\phi_s$  in the NCL regime above  $T_g$  has been measured for sorbitol, the lack of significant field dependence of the NCL in sorbitol expected by the CM cannot be tested.

Like in subsection (a), the increase of  $\phi_s$  on decreasing frequency exhibited by the two curves in the inset is assumed to be the consequence of increasing heterogeneity and number of correlated molecules in the sequence of processes following the primitive relaxation in time. If this assumption is valid, the observed increase of  $\phi_s$  in sorbitol is consistent with the interpretation of the nature of the JG  $\beta$ -relaxation in the CM. A maximum of  $\phi_s$  at 270 K is found at 2 or 3 Hz. This phenomenon is due to proximity of this frequency to the  $\alpha$ -loss peak frequency,  $f_\alpha$ . The maximum of  $\Delta \log \epsilon''(E, f)$  at frequency more than a decade higher than  $f_\alpha$  is observed in PC as shown by the inset of Fig. 3 herein and in glycerol by Fig. 2 of Bauer.<sup>8</sup> This phenomenon occurring as  $f_\alpha$  is approached is



common, but its origin is different from the nonlinear effects considered in this paper, and does not need any explanation from the CM.

### III. INVARIANCE OF THE FREQUENCY DISPERSION OF $\chi_1$ AND $\chi_3$ UNDER ISOCHRONAL CONDITION

In the effort to determine experimentally, the correlation lengths  $L_c$  or the number of correlated molecules  $N_c$  of glassformers, an advance was made by the demonstration that the third-order susceptibility,  $\chi_3(f)$ , is directly related to the four-point correlation function and hence  $L_c$ .<sup>13,68</sup> This result was put into practice to determine  $\chi_3(f)$  by dielectric spectroscopy in glycerol first by Crauste-Thibierge *et al.*<sup>2</sup> and Brun *et al.*<sup>3</sup> Recently, nonlinear dielectric measurements of  $\chi_3(f)$  were made in four different molecular glassformers, glycerol, PC, 3-fluoroaniline, and 2-ethyl-1-hexanol by Bauer *et al.*<sup>8</sup> The amplitude of the quantity  $X = |\chi_3| k_B T / [(\Delta\epsilon)^2 a^3 \epsilon_0]$  was considered in Refs. 13 and 68 to be proportional to the number of correlated molecules  $N_c$ . In this expression,  $\Delta\epsilon$  is the relaxation strength obtained from  $\chi_1(f)$ ,  $a^3$  the volume occupied by a single molecule, and  $\epsilon_0$  the permittivity of free space. Indeed, the  $N_c$  obtained from the peak amplitude of  $X$  increases with decreasing temperature in glycerol and PC.<sup>8</sup> For glycerol, the findings are similar to that of Ref. 2.

Nonlinear dielectric experiment at elevated hydrostatic pressures was performed by Casalini *et al.*<sup>11</sup> to measure  $\chi_3(f)$  of PC, corresponding to nonlinear polarization cubic in the applied electric field. They found the frequency dispersion of  $\chi_3(f)$  depends primarily on the  $\alpha$ -relaxation time and is independent of temperature  $T$  and pressure  $P$ . This is an important experimental finding of another property of  $\chi_3(f)$ , and addressing it by the CM is the other objective of this paper.

This property of  $\chi_3(f)$  is the exact analogue of the same one of the linear susceptibility  $\chi_1(f)$ . The latter is a general property found in many molecular and polymeric glass-formers.<sup>24–27,44,46–48,67</sup> Shown in numerous glassformers by dielectric relaxation and in a few by photon correlation spectroscopy is the invariance of the frequency dispersion of the  $\alpha$ -relaxation (or the value of the stretch exponent  $(1-n)$  of the Kohlrausch function) to variations of  $P$  and  $T$  while keeping  $\tau_\alpha(T, P)$  constant.<sup>23–27,44,46–48,67</sup> This remarkable property indicates that the frequency dispersion or  $(1-n)$  at any fixed  $\tau_\alpha(T, P)$  is independent of thermodynamic conditions, and solely determined by the many-body dynamics governed by the intermolecular potential. From the co-invariance of  $(1-n)$  and  $\tau_\alpha(T, P)$ , the CM equation (2) requires that  $\tau_0(T, P)$  is also invariant to variations of  $P$  and  $T$ . This formal result has support from experiments on glassformers having a resolved JG  $\beta$ -relaxation, with its relaxation time  $\tau_{JG}(T, P)$  approximately equal to  $\tau_0(T, P)$ .<sup>22–27,30</sup> It turns out that the relaxation time,  $\tau_{JG}(T, P)$ , deduced either directly from the frequency of the loss maximum, or by a fit to an empirical function, is also approximately another co-invariant together with  $(1-n)$  and  $\tau_\alpha(T, P)$ .<sup>23–27,44,46–48,67</sup> The remarkable property of co-invariance of  $\tau_\alpha(T, P)$ ,  $(1-n)$ , and  $\tau_0(T, P) \approx \tau_{JG}(T, P)$  is automatically valid for glassformers which have no resolved secondary relaxation.<sup>23,48</sup> This is because the entire frequency dispersion, including not only

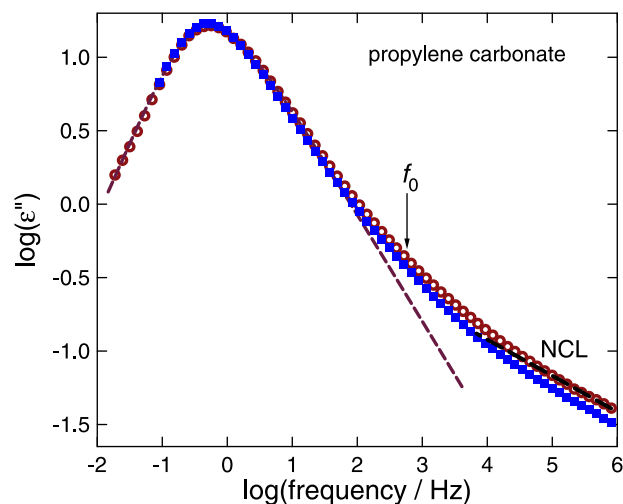


FIG. 8. Example of invariance of the frequency dispersion of the Kohlrausch  $\alpha$ -relaxation together with the faster process to variations of pressure and temperature while keeping  $f_{\max} = 0.51$  Hz or  $\tau_\alpha$  constant. The data for PC at  $T = 274.2$  K and  $P = 1.78$  GPa, and at  $T = 162.2$  K and  $P = 0.1$  MPa are taken from Ref. 48 and redrawn as a new figure. The arrow indicates the location of the primitive relaxation frequency. The dashed black line indicates the NCL at higher frequencies.

the  $\alpha$ -relaxation but also the processes at higher frequencies, is invariant to changes of  $P$  and  $T$  at constant  $\tau_\alpha(T, P)$ . An example of this property from PC is given in Fig. 8 for two combinations of  $P$  and  $T$ , where the fit of the  $\alpha$ -loss peaks of  $\chi_1(f)$  is by the Fourier transform of the Kohlrausch function with  $(1-n) = 0.73$ , and the arrow indicates the calculated primitive relaxation frequency,  $f_0(T, P)$ . Found not only at constant  $\tau_\alpha(T, P)$  in PC but also in many other non-associated glassformers without a resolved secondary relaxation such as KDE, PCB62, and salol,<sup>23,47,48</sup> the entire frequency dispersion of  $\chi_1(f)$  obeys isochronal superpositioning independent of the thermodynamic condition, and hence it is solely determined by the intermolecular interaction potential. This property is demonstrated for PC in Fig. 8 where the entire frequency dispersion, including the NCL and the intermediate relaxation processes (i.e., the unresolved JG  $\beta$ -relaxation) before reaching the terminal  $\alpha$ -relaxation, are unchanged for different combinations of  $P$  and  $T$ . The dielectric strengths of these processes do not necessarily have to change exactly by the same amount on varying  $P$  and  $T$ . This fact is the cause of the slight difference of  $\epsilon''$  of the processes at higher frequencies, when the heights of the  $\alpha$ -loss peaks are normalized to be the same. This property of dielectric  $\chi_1(f)$  should be carried over to other linear correlation functions such as in photon correlation spectroscopy as verified in Ref. 23, and also to the third order susceptibility,  $\chi_3(f)$ . This conclusion is reached simply because all linear as well as nonlinear responses are solely governed by the intermolecular potential at a fixed value of  $\tau_\alpha(T, P)$ , independent of  $T$  and  $P$ .

Reproduced in Fig. 9 are the data of  $\chi_3(f)$  taken on PC by Casalini *et al.*,<sup>11</sup> at two different combinations of  $P$  and  $T$  which have the same  $\alpha$ -loss peak frequency  $f_p$  (or the same  $\tau_\alpha$ ) in the spectra of  $\chi_1(f)$  shown in Fig. 8. The arrow indicates the location of the calculated primitive relaxation frequency,

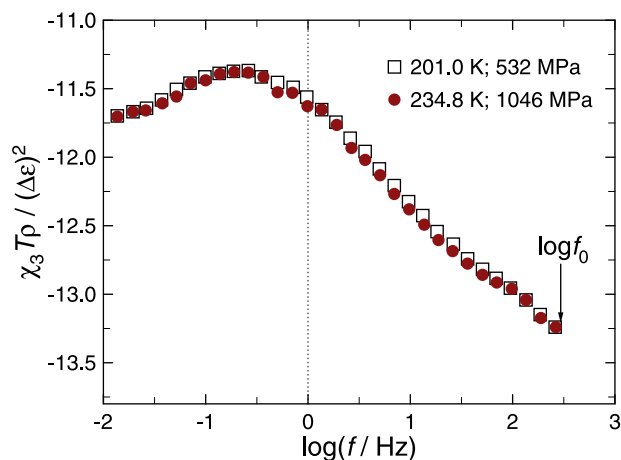


FIG. 9. Data of  $|\chi_3|T\rho/(\Delta\epsilon)^2$  digitized from a figure in Ref. 11 with additions of the calculated primitive relaxation frequencies indicated by the arrow. The present figure shows the  $|\chi_3(f)|$  spectra of PC measured at two combinations of  $P$  and  $T$ , (201.0 K, 532 MPa) and (234.8 K, 1046 MPa). Isochronal superposition is observed for the nonlinear  $|\chi_3(f)|$  of PC, as well as the linear  $\chi_1(f)$  shown before in Fig. 8.

$f_0$ . Isochronal superpositioning of the two  $\chi_3(f)$  spectra is fulfilled for all processes at frequencies below  $f_0$ .

Casalini *et al.*<sup>11</sup> carried out non-linear dielectric measurements under high pressure also on PG, which is hydrogen-bonded. It is well documented in two reviews<sup>23,30</sup> that high pressure combined with high temperature tends to break hydrogen bonds and changes the structure of the hydrogen bonded glassformers in general. Thus, the linear  $\chi_1(f)$  as well as the nonlinear  $\chi_3(f)$  of hydrogen-bonded glassformers is not invariant to changes of  $P$  and  $T$  at constant  $\tau_\alpha$ , as Casalini *et al.* found in  $\chi_3(f)$  of PG.

Without resorting to any theory for explanation, the result in Figs. 8 and 9 simply says that  $P$  and  $T$  play no role in determining the linear and the nonlinear frequency dispersions of the processes under the isochronal condition of  $\tau_\alpha$ . In the CM it is the intermolecular potential that governs all the processes including the NCL of caged molecules, and the evolution of many-body relaxation from the primitive relaxation to the terminal  $\alpha$ -relaxation. The time-scales and frequency dispersions of these chronologically ordered processes are completely determined after the constant value of  $\tau_\alpha$  or  $\tau_0$  has been specified, and hence they are invariant to changes of  $P$  and  $T$ . Theoretically, this property has a rationalization from Eq. (2) of the CM, which requires co-invariance of  $\tau_\alpha(T, P)$ ,  $(1 - n)$ , and  $\tau_0(T, P)$  to variations of  $P$  and  $T$  under isochronal condition of either  $\tau_\alpha$  or  $\tau_0$ . This rationalization is passed on to co-invariance of  $\tau_\alpha(T, P)$ ,  $(1 - n)$ , and  $\tau_{\text{JG}}(T, P)$  to variations of  $P$  and  $T$  under isochronal condition, albeit the co-invariance is only approximate as far as  $\tau_{\text{JG}}$  is concerned because of  $\tau_0(T, P) \approx \tau_{\text{JG}}(T, P)$ . More details and support from experimental data and simulations can be found in Refs. 23–27, 44, 46–48, and 67.

The time-scales and frequency dispersions of all the processes starting from the primitive relaxation to the terminal  $\alpha$ -relaxation are completely determined at constant value of either  $\tau_\alpha$  or  $\tau_0$  and independent of  $P$  and  $T$  holds not only for the linear susceptibility  $\chi_1(f)$  but also for the

third-order susceptibility,  $\chi_3(f)$ . This is because the same sequence of processes, which do not depend on  $P$  and  $T$ , is probed in the case of  $\chi_3(f)$  albeit nonlinearly. The frequency dispersions of  $\chi_3(f)$  shown in Fig. 9, cover the spectral range from the primitive relaxation to the terminal Kohlrausch  $\alpha$ -relaxation. Thus, the observed invariance of the entire frequency dispersion of  $\chi_3(f)$ , to variations of the combinations of  $P$  and  $T$  under isochronal condition, is reaffirmed by the same found in the frequency dispersion of  $\chi_1(f)$ , and the same explanation from the CM applies.

Bouchaud and Biroli<sup>13</sup> show that  $\chi_3(f)$  directly provides results of the cooperative length  $l$  and hence  $N_c$ , which are related to the dynamic heterogeneity of the  $\alpha$ -relaxation. Worthwhile to stress here is that  $N_c$  and dynamic heterogeneity, as well as non-exponentiality quantified by the Kohlrausch-Williams-Watt (KWW) correlation function, are altogether parallel consequences of the many-body relaxation dynamics of the  $\alpha$ -relaxation. The finding of the invariance of the frequency dispersion of  $\chi_3(f)$ , and hence  $N_c$  or dynamics heterogeneity, on varying  $P$  and  $T$  while keeping  $\tau_\alpha$  constant is again a consequence of the many-body relaxation governed by the intermolecular potential, in parallel with the invariance of the frequency dispersion of  $\chi_1(f)$  or the stretch exponent  $(1 - n)$  of the KWW correlation function. These properties of  $\chi_3(f)$ ,  $N_c$ , and dynamic heterogeneity are consistent with the corresponding properties of  $\chi_1(f)$  because they are parallel consequences of the many-body relaxation, but neither one controls nor is a consequence of the other.

Breakdowns of the Stokes-Einstein (SE) and the Debye-Stokes-Einstein (DSE) relations are the other experimental facts<sup>42,69,70</sup> observed in parallel with dynamic heterogeneity.<sup>71</sup> For several decades, dynamic heterogeneity of the  $\alpha$ -relaxation has been considered to have explained the observed breakdown of the SE and DSE relations.<sup>69,71</sup> Notwithstanding, dielectric, light scattering experiments, and NMR<sup>72–76</sup> have shown in three archetypal glassformers, *ortho*-terphenyl, tri-naphthal benzene, and sucrose benzoate that the frequency dispersion of the  $\alpha$ -relaxation does not change on lowering temperature from the onset temperature  $T_B$  of the breakdown and down to  $T_g$ . Hence, the dynamic heterogeneity does not change on lowering temperature towards  $T_g$  in these glassformers and cannot explain the increasing departure of translational diffusion from either viscosity or rotational dielectric relaxation.<sup>42,69</sup> The failure of using dynamic heterogeneity to explain the breakdown of SE and DSE relations has been acknowledged in a recent review.<sup>71</sup> The reason for the failure is because dynamic heterogeneity and breakdown of SE and DSE relations are parallel consequences, but it is not necessary that the former can explain the latter or vice versa.

On the other hand, the alternative explanation from the many-body  $\alpha$ -relaxation in the CM,<sup>42</sup> is based on the fact that the correlation function of translation diffusion (i.e., the mean-squared-displacement of the center of mass) is different from viscosity (a tensor), dielectric relaxation (1st order Legendre polynomial), and light scattering (2nd order Legendre polynomial). Hence, the corresponding coupling parameters to these correlation functions are different, and the difference in the  $T$ -dependence of the correlation times follow from Eq. (2).<sup>42</sup> Reference 77 further demonstrates that

the explanation<sup>42</sup> remains valid in view of the new revelations from experiments.<sup>72–76</sup>

Another study supporting the dynamic heterogeneity and the non-exponentiality parameter,  $(1 - n)$ , are parallel consequences of many-body relaxation is the molecular dynamics simulation of the Kob-Andersen binary Lennard-Jones (LJ) systems.<sup>78,79</sup> A four-point, time-dependent correlation function is required to describe dynamic heterogeneities.<sup>80,81</sup> The susceptibility  $\chi_4(t)$  defined in terms of the four-point spatial and temporal correlations has a maximum at  $t \sim \tau$  that is proportional to  $N_c$ , the number of correlating molecules<sup>82–84</sup> with

$$N_c = \max \{ \chi_4(t) \} \equiv \chi_4^{\max}. \quad (4)$$

The molecular dynamics simulations<sup>78</sup> were able to obtain the four-point correlation function, and from which the full  $t$ -dependence of  $\chi_4(t)$  and the maximum value  $\chi_4^{\max}(=N_c)$  were obtained and found invariant over a relevant range of  $T$  and  $\rho$  for state points for which the scaling variable  $\rho^\gamma/T$  is constant with  $\gamma = 5.07$ . Moreover, the reduced relaxation time  $\tau^*$ , defined as the Kohlrausch decay time for the intermediate scattering function  $F(k, t)$  is also invariant for state points for which  $\rho^\gamma/T$  is constant with  $\gamma = 5.07$ . Thus, the same value of the material constant  $\gamma = 5.07$  superposes both  $\chi_4^{\max}$  and  $\tau^*$  of the system versus  $\rho^\gamma/T$ , which means that  $N_c$  is a unique function of  $\tau^*$ , in the regime where density scaling holds.

The results for  $\beta_K \equiv (1 - n)$  were obtained in Ref. 79 by fitting the intermediate scattering function  $F(k, t)$  over the same range of  $T$  and  $\rho$  as in Ref. 78. It was found that  $\beta_K$  also is a function of  $\rho^\gamma/T$  using  $\gamma = 5.07$ , the same exponent superposing  $\chi_4^{\max}$  versus  $\rho^\gamma/T$ . Thus,  $\beta_K$  is invariant for state points at which the scaling variable  $\rho^\gamma/T$  is constant with  $\gamma = 5.07$ . The results indicate that  $\beta_K$ , like the full  $t$ -dependence of  $\chi_4(t)$  or the maximum value,  $\chi_4^{\max}(=N_c)$ , is a unique function of  $\tau^*$  under any thermodynamic condition in the regime where density scaling holds. Therefore, from the molecular dynamics simulations we had reached before in Ref. 79 similar conclusion as the invariance of the frequency dispersions of  $\chi_3(f)$  ( $\propto N_c$ ) for PC by Casalini *et al.*<sup>11</sup> on varying  $P$  and  $T$  while keeping  $\tau_\alpha$  constant. It is perfectly clear that the molecular dynamics simulations<sup>78</sup> start from the intermolecular LJ potential. All the quantities obtained, including  $\beta_K$  and  $\chi_4(t)$  or  $\chi_4^{\max}(=N_c)$ , and their properties of invariance at constant  $\tau^*$  under any thermodynamic condition, are all parallel consequences of the many-body relaxation governed by the potential. Therefore, it is not possible to take one of the parallel consequences, such as  $N_c$  or dynamic heterogeneity, and consider it as the principal control parameter of the dynamics of glassforming systems as suggested in Ref. 11. For example, we have already shown dynamic heterogeneity cannot explain the breakdown of SE and DSE relations, despite the fact that they are both present in *ortho*-terphenyl, trinaphthal benzene, and sucrose benzoate.

#### IV. CONCLUSIONS

The experimental studies of nonlinear dielectric response of glassformers are primarily intended to understand better dynamics heterogeneity, its length-scale, and the number of

correlated molecules  $N_c$  in the  $\alpha$ -relaxation as temperature is lowered towards glass transition. While this objective has been accomplished to a great extent for the  $\alpha$ -relaxation, the high-field measurements at frequencies significantly higher than the  $\alpha$ -relaxation have provided new opportunities for better understanding the nature and origin of the faster processes. In glassformers having no resolved secondary relaxation such as glycerol and PC, the faster process of interest is the EW or the unresolved JG  $\beta$ -relaxation, and even faster is the nearly NCL of caged molecules. A finding by Bauer *et al.* is that the change of dielectric loss by the high field,  $\Delta \log \varepsilon''(E, f)$ , is vanishingly small in the NCL region, which surprised them because the EW (in their nomenclature and NCL in this paper) is customarily considered as some distribution of relaxation process. This conundrum is resolved by the CM in identifying the NCL as originating from loss of molecules mutually caged via the intermolecular potential. The anharmonicity of the potential determines the magnitude of the NCL, which is not a relaxation process with a characteristic time. Since the intermolecular potential is insensitive to electric field strength, so is the NCL, and hence the lack of significant change of  $\varepsilon''(E, f)$  on applying high fields. On the other hand, the primitive relaxation and the subsequent relaxation processes involving increasing number of molecules with time are spatially and dynamically heterogeneous, and hence they show nonlinear dielectric effects measured by  $\Delta \log \varepsilon''(E, f)$ . The observed increase of  $\Delta \log \varepsilon''(E, f)$  on lowering frequency  $f$  is consistent with the increasing heterogeneity and the number of participating molecules (i.e., cooperativity) with increasing time within the context of the CM. The relative change of the dielectric loss induced by application of a high field in glycerol and PC recorded in a standard impedance mode with only moderately long measurement times by SR are consistent with the data of Bauer *et al.* In addition, SR obtained time-resolved relative change of the dielectric loss induced by high field in glycerol and PC at temperatures near  $T_g$ . However, the highest frequencies examined are either lower than or at the onset frequency of the NCL. Hence, the extant time-resolved data of SR cannot be used to estimate the size of the nonlinear dielectric effect of the NCL. On the other hand, the high field effect had been studied in glycerol at 186 K by Bauer *et al.* at frequencies much deeper inside in the NCL regime for long times corresponding to more than  $2 \times 10^5$  cycles, and no high field induced change of  $\varepsilon''$  was observed.

For glassformers having a resolved JG  $\beta$ -relaxation, according to the evolution of many-body relaxation dynamics view of the coupling model, it should not be considered as coming from an empirical distribution of relaxation times unrelated to the  $\alpha$ -relaxation, and as an independent contribution to the susceptibility to be added to the  $\alpha$ -relaxation. Instead, it is composed of the local primitive relaxation and sequentially the relaxation processes involving increasing degree of heterogeneity and number of correlated molecules, and collectively called the JG  $\beta$ -relaxation. Thus, nonlinear dielectric effects are expected to be observed in the primitive relaxation and the JG  $\beta$ -relaxation, and indeed this is confirmed by experiments in D-sorbitol.<sup>10,65</sup>

Invariance to variations of pressure and temperature of the frequency dispersion of the  $\alpha$ -relaxation at constant  $\tau_\alpha$  is



a general property of  $\chi_1(f)$  for non-associated glassformers. The property clearly indicates that frequency dispersion is not determined by  $P$  and  $T$  under isochronal condition, but rather all the evolving processes from the NCL, the JG  $\beta$ -relaxation to the  $\alpha$ -relaxation are governed by the intermolecular potential. Invariance of the  $\alpha$ -dispersion and JG  $\beta$ -relaxation (resolved or not) should hold for any susceptibility  $\chi_1(f)$  derived from various correlation functions in linear response as well as  $\chi_3(f)$  in nonlinear response according to the CM. High-field experiment performed on PC at elevated pressures under isochronal condition of  $\tau_\alpha$  has confirmed the invariance of the frequency dispersion of  $\chi_3(f)$  covering not only the  $\alpha$ -relaxation but also the faster relaxation processes including the primitive relaxation. It follows from the theoretical result given by Ref. 13 that the number of correlated molecules  $N_c$  or the dynamic heterogeneity length-scale  $L_c$  is invariant to thermodynamic conditions under isochronal conditions. Notwithstanding, this deduction should not be overextended to say  $N_c$  or dynamic heterogeneity is the principal control parameter for all the other properties of the dynamics of molecular motions in glassforming systems.<sup>11</sup> Actually, dynamic heterogeneity is one of many parallel consequences of the many-body relaxation governed by the intermolecular potential. For the  $\alpha$ -relaxation alone, the parallel consequences include the frequency dispersion (or the exponent,  $\beta_K = 1 - n$  of the Kohlrausch correlation function), dynamics heterogeneity and its length-scale  $L_c$ , the number of correlated molecules  $N_c$ , the breakdown of SE and DSE relations, and etc. The parallel consequences are consistent with each other, but it may not be possible to take one consequence and explain another parallel consequence. Support of this conclusion can be taken from molecular dynamic simulations of the Kob-Andersen's Lennard-Jones (LJ) systems, where the dynamics are determined solely by the LJ inter-particles potential, and all properties are generated as parallel consequences. The properties include  $\beta_K$ , and  $\chi_4(t)$  or  $\chi_4^{\max}(=N_c)$ , and the invariance of these parameters to thermodynamic conditions at constant  $\tau_\alpha$ , as well as the breakdown of the SE and DSE relations.

## APPENDIX: EVOLUTION OF MANY-BODY DYNAMICS WITH TIME: THE COUPLING MODEL

In the literature, current and past, there are different interpretations of the dynamic processes present over extended time/frequency range. The more familiar view of the dynamics of glassforming liquids is that they are composed of independent and additive contributions from various processes, transpiring at different time-scales. No relation between the time-scales or relaxation times, strength, and properties of the various processes is expected or predicted. On the other hand, in the CM, all relevant dynamic processes are governed by the intermolecular potential. The dynamics evolve and change with time. Starting at short times is the motion of molecules confined within cages via the intermolecular potential, and the loss is determined by anharmonicity of the potential. The caged dynamics is not a normal relaxation process. It has no characteristic time, and hence the loss is a power law,  $\chi''(f) = A(T)f^{-c}$  with  $c < 1$ , or the NCL in the susceptibility

spectrum. Neither cooperativity nor heterogeneity applies to the NCL of caged dynamics because molecules remain caged throughout the regime, and the loss originates from the anharmonicity of the potential. Although caged dynamics form the core issue of the idealized Mode Coupling Theory,<sup>17</sup> the NCL is not a prediction of it.<sup>33–37</sup> This NCL regime persists until the cages are dissolved by the onset of the primitive relaxation of the CM,<sup>28–30</sup> the motion of which involving the entire molecule (i.e., generalized analogue of the totally rigid molecules studied by Johari and Goldstein). Thus, in order of magnitude only, the primitive relaxation time,  $\tau_0(T, P)$ , is an upper bound of the NCL time regime, a prediction verified by experimental data and molecular dynamics simulations in many molecular glassformers,<sup>28–30</sup> and ionic conductors.<sup>28,43,44</sup> The weak temperature dependence of the intensity factor,  $A(T) \propto \exp(T/T_0)$ , where  $T < T_0$  is also derivable from the primitive relaxation frequency,  $f_0(T, P) \equiv 2\pi/\tau_0(T, P)$ , acting as the lower bound of the NCL frequency regime.<sup>43</sup> The primitive relaxation involving individual molecules is the start of the evolution of the relaxation dynamics with time that involves increasing number of molecules. If some feature in the dielectric loss spectrum, showing up either as a resolved maximum or shoulder near the primitive frequency,  $f_0(T, P)$ , it is customarily identified as the JG  $\beta$ -relaxation. Often a Cole-Cole function is used to fit the observed feature and the entire function is considered to represent the JG  $\beta$ -relaxation, and its relaxation frequency  $f_{JG}(T, P)$  or time  $\tau_{JG}(T, P)$  is determined from the fit. This practice assumes that the JG  $\beta$ -relaxation makes a contribution to the susceptibility that is independent of and additive to the  $\alpha$ -relaxation. However, this is contradicted by the many experimental facts indicating the JG  $\beta$ -relaxation is connected to the NCL and related to the  $\alpha$ -relaxation, and it cannot be considered as an independent and additive contribution to either processes.<sup>16,21–30</sup> In many cases, where the feature in the loss spectrum is not prominent, such as a shoulder or a very broad peak but suggesting the presence of the JG  $\beta$ -relaxation, the Cole-Cole function used to fit it is so broad that its low frequency flank overlaps the much narrower  $\alpha$ -relaxation peak. The situation is unphysical because it is inconceivable that the precursory JG  $\beta$ -relaxation can continue to have contributions at times longer than the  $\alpha$ -relaxation time  $\tau_\alpha(T, P)$ . Thus, the common view of the JG  $\beta$ -relaxation is questionable.

The view from the CM is different. The local primitive relaxation is definitely a non-cooperative relaxation and its correlation function is the exponential function,  $\phi(t) = \exp(-t/\tau_0)$ .<sup>27–30</sup> Nonetheless, it can occur anywhere involving different molecules stochastically, and hence it is spatially heterogeneous. In the susceptibility spectrum, the onset of the primitive relaxation is followed in time by spatially heterogeneous relaxation processes involving increasing number of molecules. The collection of these processes is identified as the JG  $\beta$ -relaxation. This evolution of many-body relaxation dynamics continues with time until the maximum number  $N_c$  allowed by the intermolecular potential has been reached in forming the  $\alpha$ -relaxation with the correlation function of Kohlrausch (Eq. (1)). The ToC of the perspective<sup>44</sup> serves as a pictorial illustration of the CM view of the sequential time evolution in the order of NCL, the primitive relaxation, the

JG  $\beta$ -relaxation resolved or unresolved, and the  $\alpha$ -relaxation. It is necessary to make this CM view explicit in here. This is because this view is not the same as that of Bauer *et al.*<sup>7</sup> on the nature of the EW in considering the nonlinear dielectric effect, in linear response as that of the idealized MCT<sup>17</sup> of caged dynamics, and other workers on dynamics of glassformers. For example, a marked difference in view from the CM is given by authors of Ref. 32(b). For glassformers showing no resolved secondary relaxation including glycerol and propylene carbonate, they proposed the succession of processes appearing in the loss spectra on increasing frequency are the  $\alpha$ -relaxation, an excess wing, and the  $\beta$ -relaxation. This proposal is evident from their Fig. 5 in Ref. 32(b).

Buchenau *et al.*<sup>61</sup> proposed that fragility of the  $\alpha$ -relaxation is determined by the combined effect of anharmonicity and the Adam-Gibbs mechanism of a growing cooperatively rearranging region. Their proposal is along the same line as a previous work,<sup>85</sup> which had recognized the transition rate of the cooperative rearranging regions in the Adam-Gibbs model does not capture all the complexities of the many-body molecular motion caused by intermolecular interaction. It was modified by combining it with the CM equation (2) to construct a modified model with predictions consistent with several experimental data sets and phenomena including fragility. The modification is principally via the coupling parameter  $n$  in Eq. (2), which is determined by the anharmonicity of the potential. Thus, the proposal by Buchenau *et al.* has the same spirit as was done before in Ref. 85. They also proposed that nonlinear dielectric experiments do not measure  $N_c$  alone, but rather the barrier height itself, together with its anharmonic changes. The emphasis on anharmonicity of the potential by Buchenau *et al.* in nonlinear response is limited to the  $\alpha$ -relaxation. On the other hand, the CM considers the intermolecular potential governing all linked processes: caged dynamics, the primitive and the JG  $\beta$ -relaxation, and the  $\alpha$ -relaxation. Anharmonicity of the potential gives rise to chaos which in turn determines the characteristics of these processes and their relations.<sup>30,40</sup> This view of the CM has support from the experimental results obtained on colloidal particles suspension with volume fraction of 0.56 from the confocal microscopy experiment by Weeks *et al.*<sup>63,64</sup> This spectroscopy has the advantage that motions of all colloidal particles can be observed continuously as a function of time, and hence the evolution of dynamics can be compared with the CM. In a suspension with volume fraction of particles equal to 0.56, a typical particle takes average time of 500 s to shift position and leave the cage. This time is identifiable with the primitive relaxation time  $\tau_0$  of the CM. At times shorter than 200 s, the mean square displacements,  $\langle x^2(t) \rangle$ , is proportional to  $t^c$  with  $c \approx 0.13$ , corresponding to the NCL of caged dynamics, which is terminated at 500 s by the onset of the single particle jump or the primitive relaxation. Ref. 64 demonstrated further that the cage is decayed by local jumps of particles, the analogue of the primitive relaxation as clearly shown in Ref. 30. Beyond  $\tau_0 = 500$  s, the confocal microscopy experiment shows spatially and dynamically heterogeneous relaxation involving more particles. The number of particles increases with time until  $\langle x^2(t) \rangle$  becomes proportional to  $t$ , which corresponds to viscous flow associated

with the  $\alpha$ -relaxation in molecular glassformers. A molecular dynamics simulation of dynamics of ions in a Li metasilicate glass also found the same properties as the colloidal particles.<sup>55</sup>

The confocal microscopy data of colloidal particles show there is no single process that can be identified in the intermediate time regime between caged dynamics and steady state diffusion. The result indicates that representing the so-called JG  $\beta$ -relaxation by any empirical function such as Cole-Cole and considered it to be an additive contribution to the  $\alpha$ -relaxation is not the way to understand the dynamics of glassformers. Notwithstanding, this common practice is the convenient way to provide a characteristic time  $\tau_{JG}(T, P)$ . It is artificial and hence the value of  $\tau_{JG}(T, P)$  obtained this way can only serve as an order of magnitude estimate of  $\tau_0(T, P)$ , i.e.,  $\tau_{JG}(T, P) \approx \tau_0(T, P)$ . On the other hand,  $\tau_0(T, P)$  can be obtained from the parameters  $\tau_\alpha(T, P)$  and  $(1 - n)$  of the Kohlrausch function via the coupling model Eq. (2). Through the calculated  $\tau_0(T, P)$  and  $\tau_{JG}(T, P) \approx \tau_0(T, P)$ , the existence of multiple connections between the JG  $\beta$ -relaxation and the  $\alpha$ -relaxation has been demonstrated from experimental data starting from 1998<sup>16</sup> till nowadays.<sup>22–30,44,46–48</sup> These connections support the fundamental importance of the primitive or the JG  $\beta$ -relaxation.

<sup>1</sup>R. Richert and S. Weinstein, *Phys. Rev. Lett.* **97**, 095703 (2006).

<sup>2</sup>C. Crauste-Thibierge, C. Brun, F. Ladieu, D. L'Hôte, G. Biroli, and J.-P. Bouchaud, *Phys. Rev. Lett.* **104**, 165703 (2010).

<sup>3</sup>C. Brun, F. Ladieu, D. L'Hôte, M. Tarzia, G. Biroli, and J.-P. Bouchaud, *Phys. Rev. B* **84**, 104204 (2011).

<sup>4</sup>C. Brun, C. Crauste-Thibierge, F. Ladieu, and D. L'Hôte, *J. Chem. Phys.* **134**, 194507 (2011).

<sup>5</sup>S. J. Rzoska and A. Drozd-Rzoska, *J. Phys.: Condens. Matter* **24**, 035101 (2012).

<sup>6</sup>L.-M. Wang and R. Richert, *Phys. Rev. Lett.* **99**, 185701 (2007).

<sup>7</sup>Th. Bauer, P. Lunkenheimer, S. Kastner, and A. Loidl, *Phys. Rev. Lett.* **110**, 107603 (2013), see also the supplementary information.

<sup>8</sup>T. Bauer, P. Lunkenheimer, and A. Loidl, *Phys. Rev. Lett.* **111**, 225702 (2013).

<sup>9</sup>S. Samanta and R. Richert, *J. Chem. Phys.* **140**, 054503 (2014).

<sup>10</sup>S. Samanta and R. Richert, "Nonlinear dielectric behavior of a secondary relaxation: Glassy D-sorbitol," *J. Phys. Chem. B* (to be published).

<sup>11</sup>R. Casalini, D. Fragiadakis, and C. M. Roland, "Dynamic correlation length scales under isochronal conditions," e-print [arXiv:1410.0625](https://arxiv.org/abs/1410.0625) (2014).

<sup>12</sup>J. L. Déjardin and Yu. P. Kalmykov, *Phys. Rev. E* **61**, 1211 (2000).

<sup>13</sup>J.-P. Bouchaud and G. Biroli, *Phys. Rev. B* **72**, 064204 (2005).

<sup>14</sup>G. Diezemann, *Phys. Rev. E* **85**, 051502 (2012).

<sup>15</sup>S. Weinstein and R. Richert, *Phys. Rev. B* **75**, 064302 (2007).

<sup>16</sup>K. L. Ngai, *J. Chem. Phys.* **109**, 6982 (1998).

<sup>17</sup>W. Götze, *J. Phys.: Condens. Matter* **11**, A1 (1999).

<sup>18</sup>P. Lunkenheimer, U. Schneider, R. Brand, and A. Loidl, *Contemp. Phys.* **41**, 15 (2000).

<sup>19</sup>R. Böhmer, G. Diezemann, B. Geil, G. Hinze, A. Nowaczyk, and M. Winterlich, *Phys. Rev. Lett.* **97**, 135701 (2006).

<sup>20</sup>U. Schneider, R. Brand, P. Lunkenheimer, and A. Loidl, *Phys. Rev. Lett.* **84**, 5560 (2000).

<sup>21</sup>A. Döb, M. Paluch, H. Sillescu, and G. Hinze, *Phys. Rev. Lett.* **88**, 095701 (2002).

<sup>22</sup>K. L. Ngai and M. Paluch, *J. Chem. Phys.* **120**, 857 (2004).

<sup>23</sup>K. L. Ngai, R. Casalini, S. Capaccioli, M. Paluch, and C. M. Roland, *Advances in Chemical Physics, Part B* (John Wiley & Sons, 2006), Vol. 133, Chap. 10, p. 497.

<sup>24</sup>M. Mierzwa, S. Pawlus, M. Paluch, E. Kaminska, and K. L. Ngai, *J. Chem. Phys.* **128**, 044512 (2008).

<sup>25</sup>K. Kessairi, S. Capaccioli, D. Prevosto, M. Lucchesi, S. Sharifi, and P. A. Rolla, *J. Phys. Chem. B* **112**, 4470 (2008).

<sup>26</sup>D. Bedrov and G. D. Smith, *J. Non-Cryst. Solids* **357**, 258 (2011).

<sup>27</sup>K. L. Ngai, J. Habasaki, D. Prevosto, S. Capaccioli, and M. Paluch, *J. Chem. Phys.* **137**, 034511 (2012).

- <sup>28</sup>K. L. Ngai, *J. Phys.: Condens. Matter* **15**, S1107 (2003).
- <sup>29</sup>S. Capaccioli, M. S. Thayyil, and K. L. Ngai, *J. Phys. Chem. B* **112**, 16035 (2008).
- <sup>30</sup>K. L. Ngai, *Relaxation and Diffusion in Complex Systems* (Springer, NY, 2011).
- <sup>31</sup>S. Kastner, M. Köhler, Y. Goncharov, P. Lunkenheimer, and A. Loidl, *Non-Cryst. Solids* **357**, 510 (2011).
- <sup>32</sup>(a) C. Gainaru, A. Rivera, S. Putselyk, G. Eska, and E. A. Rössler, *Phys. Rev. B* **72**, 174203 (2005); (b) C. Gainaru, R. Kahlau, E. A. Rössler, and R. Böhmer, *J. Chem. Phys.* **131**, 184510 (2009).
- <sup>33</sup>G. Hinze, D. D. Brace, S. D. Gottke, and M. D. Fayer, *J. Chem. Phys.* **113**, 3723 (2000).
- <sup>34</sup>A. P. Sokolov, A. Kisluk, V. N. Novikov, and K. Ngai, *Phys. Rev. B* **63**, 172204 (2001).
- <sup>35</sup>S. D. Gottke, D. D. Brace, G. Hinze, and M. D. Fayer, *J. Phys. Chem.* **105**, 238 (2001).
- <sup>36</sup>A. Kisluk, V. N. Novikov, and A. P. Sokolov, *J. Polym. Sci., Part B: Polym. Phys.* **40**, 201 (2002).
- <sup>37</sup>H. Cang, V. N. Novikov, and M. D. Fayer, *J. Chem. Phys.* **118**, 2800 (2003).
- <sup>38</sup>M. Köhler, P. Lunkenheimer, Y. Goncharov, and A. Loidl, *Phys. Rev. E* **87**, 062320 (2013).
- <sup>39</sup>G. P. Johari and M. Goldstein, *J. Chem. Phys.* **53**, 2372 (1970).
- <sup>40</sup>K. L. Ngai, Comment, *Solid State Phys.* **9**, 141 (1979); K. Y. Tsang and K. L. Ngai, *Phys. Rev. E* **54**, R3067 (1996); **56**, R17 (1997); K. L. Ngai and K. Y. Tsang, *ibid.* **60**, 4511 (1999).
- <sup>41</sup>Y. Cohen, S. Karmakar, I. Procaccia, and K. Samwer, *Europhys. Lett.* **100**, 36003 (2012).
- <sup>42</sup>K. L. Ngai, *J. Phys. Chem. B* **103**, 10684-10694 (1999). It was made clear in this paper that the  $\alpha$ -relaxation in the CM is dynamically heterogeneous. Nevertheless the emphasis of the wide application of the CM equation (2) between  $\tau_\alpha$  and  $\tau_0$  in publications can give others a false impression that the  $\alpha$ -relaxation is homogeneous in the CM. This happened before in the review article by H. Sillescu, *J. Non-Cryst. Solids* **243**, 81 (1999). This misunderstanding by him was recognized later and rectified in a follow-up review, R. Böhmer, G. Hinze, G. Diezemann, B. Geil, H. Sillescu, *Europhys. Lett.* **36**, 55 (1996), coauthored by Sillescu. The review by M. D. Ediger [*Annu. Rev. Phys. Chem.* **51**, 99 (2000)] also had mistaken the CM as homogeneous.
- <sup>43</sup>(a) K. L. Ngai, J. Habasaki, Y. Hiwatari, and C. León, *J. Phys.: Condens. Matter* **15**, S1607-S1632 (2003); (b) C. León, K. L. Ngai, and A. Rivera, *Phys. Rev. B* **69**, 134303 (2004); (c) K. L. Ngai, *Philos. Mag.* **84**, 1341-1353 (2004); (d) A. Rivera, C. León, J. Sanz, J. Santamaría, C. T. Moynihan, and K. L. Ngai, *Phys. Rev. B* **65**, 224302 (2004); (e) G. Jarosz, M. Mierzwa, J. Ziolo, M. Paluch, H. Shirota, and K. L. Ngai, *J. Phys. Chem. B* **115**, 12709 (2011).
- <sup>44</sup>S. Capaccioli, M. Paluch, D. Prevosto, L.-M. Wang, and K. L. Ngai, *J. Phys. Chem. Lett.* **3**, 735 (2012).
- <sup>45</sup>A. Nowaczyk, B. Geil, G. Hinze, and R. Böhmer, *Phys. Rev. E* **74**, 041505 (2006).
- <sup>46</sup>K. L. Ngai, *AIP Conf. Proc.* **1518**, 18 (2013).
- <sup>47</sup>C. M. Roland, R. Casalini, and M. Paluch, *Chem. Phys. Lett.* **367**, 259-264 (2003).
- <sup>48</sup>K. L. Ngai, R. Casalini, S. Capaccioli, M. Paluch, and C. M. Roland, *J. Phys. Chem. B* **109**, 17356-17360 (2005).
- <sup>49</sup>(a) K. Schmidt-Rohr and H. W. Spiess, *Phys. Rev. Lett.* **66**, 3020 (1991); (b) U. Tracht, M. Wilhelm, A. Heuer, H. Feng, K. Schmidt-Rohr, and H. W. Spiess, *Phys. Rev. Lett.* **81**, 2727 (1998); (c) S. A. Reinsberg, A. Heuer, B. Doliwa, H. Zimmermann, and H. W. Spiess, *J. Non-Cryst. Solids* **307-310**, 208 (2002).
- <sup>50</sup>B. Schiener, R. V. Chamberlin, G. Diezemann, and R. Böhmer, *J. Chem. Phys.* **107**, 7746 (1997).
- <sup>51</sup>R. Richert and R. Böhmer, *Phys. Rev. Lett.* **83**, 4337 (1999).
- <sup>52</sup>R. Richert, *Europhys. Lett.* **54**, 767 (2001).
- <sup>53</sup>K. Duvvuri and R. Richert, *J. Chem. Phys.* **118**, 1356 (2003).
- <sup>54</sup>Z. Wojnarowska, K. Kołodziejczyk, K. J. Paluch, L. Tajber, K. Grzybowska, K. L. Ngai, and M. Paluch, *Phys. Chem. Chem. Phys.* **15**, 9205 (2013).
- <sup>55</sup>J. Habasaki and K. L. Ngai, *J. Non-Cryst. Solids* **352**, 5170-5177 (2006).
- <sup>56</sup>T. Blochowicz and E. A. Rössler, *Phys. Rev. Lett.* **92**, 225701 (2004).
- <sup>57</sup>K. L. Ngai, P. Lunkenheimer, C. León, U. Schneider, R. Brand, and A. Loidl, *J. Chem. Phys.* **115**, 1405 (2001).
- <sup>58</sup>A. Kudlik, S. Benkhof, T. Blochowicz, C. Tschirwitz, and E. Rössler, *J. Mol. Struct.* **479**, 201 (1999).
- <sup>59</sup>Th. Bauer, P. Lunkenheimer, and A. Loidl, private communication (2014).
- <sup>60</sup>K. L. Ngai, *J. Non-Cryst. Solids* **275**, 7 (2000).
- <sup>61</sup>U. Buchenau, R. Zorn, and M. A. Ramos, *Phys. Rev. E* **90**, 042312 (2014).
- <sup>62</sup>S. Gupta, N. Arend, P. Lunkenheimer, A. Loidl, L. Stingaciu, N. Jalarvo, E. Mamontov, and M. Ohl, *Eur. Phys. J. E* **38**, 1 (2015).
- <sup>63</sup>E. R. Weeks, J. C. Crocker, A. C. Levitt, A. Schofield, and D. A. Weitz, *Science* **287**, 627 (2000).
- <sup>64</sup>E. R. Weeks and D. A. Weitz, *Phys. Rev. Lett.* **89**, 095704 (2002).
- <sup>65</sup>Th. Bauer, Ph.D. thesis, University of Augsburg, Augsburg, Germany, 2014.
- <sup>66</sup>R. Nozaki, D. Suzuki, S. Ozawa, and Y. Shiozaki, *J. Non-Cryst. Solids* **235-237**, 393 (1998).
- <sup>67</sup>M. Shahin Thayyil, K. L. Ngai, D. Prevosto, and S. Capaccioli, *J. Non-Cryst. Solids* **407**, 98-105 (2014).
- <sup>68</sup>M. Tarzia, G. Biroli, A. Lefe`vre, and J.-P. Bouchaud, *J. Chem. Phys.* **132**, 054501 (2010).
- <sup>69</sup>M. K. Mapes, S. F. Swallen, and M. D. Ediger, *J. Phys. Chem. B* **110**, 507 (2006).
- <sup>70</sup>K. L. Ngai, J. H. Magill, and D. J. Plazek, *J. Chem. Phys.* **112**, 1887 (2000).
- <sup>71</sup>M. D. Ediger and P. Harrowell, *J. Chem. Phys.* **137**, 080901 (2012).
- <sup>72</sup>R. Richert, K. Duvvuri, and L. J. Duong, *J. Chem. Phys.* **118**, 1828 (2003).
- <sup>73</sup>R. Richert, *J. Chem. Phys.* **123**, 154502 (2005).
- <sup>74</sup>J. R. Rajian, W. Huang, R. Richert, and E. L. Quitevis, *J. Chem. Phys.* **124**, 014510 (2006).
- <sup>75</sup>X. R. Zhu and C. H. Wang, *J. Chem. Phys.* **84**, 6086-6090 (1986).
- <sup>76</sup>K. Zemke, K. Schmidt-Rohr, J. H. Magill, H. Sillescu, and H. W. Spiess, *Mol. Phys.* **80**, 1317-1330 (1993).
- <sup>77</sup>K. L. Ngai, *Philos. Mag.* **87**, 357-370 (2007).
- <sup>78</sup>D. Coslovich and C. M. Roland, *J. Chem. Phys.* **131**, 151103 (2009).
- <sup>79</sup>C. M. Roland, D. Fragiadakis, D. Coslovich, S. Capaccioli, and K. L. Ngai, *J. Chem. Phys.* **131**, 124507 (2010).
- <sup>80</sup>C. Dasgupta, A. V. Indrani, S. Ramaswamy, and M. K. Phani, *Europhys. Lett.* **15**, 307 (1991).
- <sup>81</sup>S. Franz and G. Parisi, *J. Phys. Condens.: Matter* **12**, 6335 (2000).
- <sup>82</sup>D. Chandler, J. P. Garrahan, R. L. Jack, L. Maibaum, and A. C. Pan, *Phys. Rev. E* **74**, 051501 (2006).
- <sup>83</sup>C. Donati, S. Franz, S. C. Glotzer, and G. Parisi, *J. Non-Cryst. Solids* **307-310**, 215 (2002).
- <sup>84</sup>C. Toninelli, M. Wyart, L. Berthier, G. Biroli, and J.-P. Bouchaud, *Phys. Rev. E* **71**, 041505 (2005).
- <sup>85</sup>K. L. Ngai, *J. Phys. Chem. B* **103**, 5895-5902 (1999).